2015 IEEE International Conference on Robotics and Automation (ICRA)
Washington State Convention Center
Seattle, Washington, May 26-30, 2015

Mixed Integer Quadratic Program Trajectory Generation for a Quadrotor with a Cable-Suspended Payload

Sarah Tang and Vijay Kumar[1]

Abstract— **In this paper, we present a trajectory planning method to navigate a quadrotor with a cable-suspended payload through known obstacle-filled environments. We model the system as a hybrid dynamical system and formulate the trajectory generation problem as a Mixed Integer Quadratic Program (MIQP). Specifically, we address two novel challenges. First, we plan for a multi-body system, and obstacle avoidance must be guaranteed for the quadrotor, load, and the cable. Second, our method accommodates transitions between subsystems of the hybrid dynamical system, allowing for maneuvers that would otherwise be infeasible if the cable were constrained to remain taut. Numerical and experimental results validate the proposed approach for the full hybrid system.**

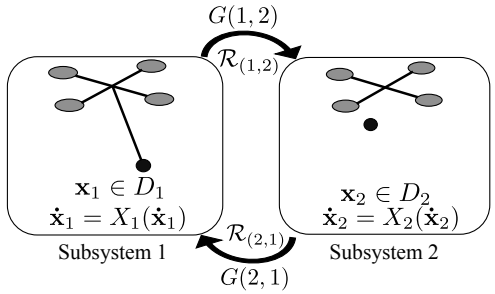

Fig. 1. Quadrotor with a cable-suspended load hybrid system

I. Introduction

Recently, unmanned aerial vehicles (UAVs), in particular quadrotors, have proven useful for many tasks, including multi-agent missions, mapping and exploration, and even acrobatic performances. They have also been used to manipulate objects for construction and transportation.

One possibility is to attach an articulated gripper to the quadrotor, which has previously been studied [1] [2]. However, connecting the payload with a cable suspension may allow the vehicle to retain more of its inherent agility. Previous work on helicopter [3] and quadrotor systems [4] with suspended loads have focused on load stabilization and minimization of the load swing while traversing trajectories. Unfortunately, this precludes the automation of tasks that require fast and aggressive load maneuvering, such as Christmas tree harvesting or extinguishing forest fires. In contrast, we hope to exploit the system's entire range of motion and consider trajectories with large load swings, load pick-ups and releases, and periods of zero cable tension where the load is in temporary free-fall.

To this end, we model our system as a hybrid dynamical system, illustrated in Fig. 1. In the "quadrotor-with-load subsystem", the cable is taut and the quadrotor is controlling the load. In the "quadrotor subsystem", the quadrotor motion is controlled while load is undergoing projectile motion. Past work has developed a nonlinear controller for load position tracking in the quadrotor-with-load subsystem with almost global stability properties [5], [6]. We build on this work by developing a trajectory planning technique for the complete hybrid system through known obstacle-filled environments.

We gratefully acknowledge the support of ARL grant W911NF-08-2-0004, ONR grants N00014-07-1-0829 and N00014-09-1-1051, and NSF grant IIS-1426840.

[1]S. Tang and V. Kumar are with the Department of Mechanical Engineering and Applied Mechanics. University of Pennsylvania, Phildadelphia, PA 19104, USA {sytang, kumar}@seas.upenn.edu

We do this with a trajectory optimization approach. In previous work, Richter et al. [7] optimize quadrotor trajectories using a Quadratic Program (QP). Mellinger et al. [8] solve a Mixed Integer Quadratic Program (MIQP) for optimal quadrotor trajectories, using integer constraints for collision avoidance. Deits et al. [9] similarly use integer constraints in a Mixed Integer Quadratically Constrained Quadratic Program (MIQCP) for footstep planning for a humanoid robot. Our work also embeds obstacle avoidance with integer constraints. However, we address the additional challenges of planning for a multi-body, hybrid dynamical system.

In related work, de Crousaz et al. [10] address planning and control for the quadrotor with payload system using an iterative LQG (iLQG) algorithm. While some example tasks are similar, our work differs in a number of ways. First, the iLQG cost function only penalizes deviation from desired states and nominal inputs, while we consider optimality for the system's dynamics. Additionally, our method only requires knowledge of the position of obstacle faces, while tuning the iLQG cost function requires the addition of terms based on human knowledge. Finally, we can explicitly impose constraints on obstacle avoidance, maximum velocities and accelerations, and motor inputs.

This paper is organized as follows. Section II describes the system dynamics and control. Section III outlines the fundamentals of our approach and Sections IV and V describe our trajectory generation method. Section VI discusses numerical examples and Section VII presents experimental results. Finally, Section VIII provides concluding remarks.

II. Dynamics and Control

Fig. 1 shows our hybrid dynamical model. Subsystem 1 refers to the quadrotor-with-load subsystem while subsystem 2 refers to the quadrotor subsystem. We treat the quadrotor as a rigid-body and the load as a point-mass. We will refer to the condition for transitioning between two subsystems as

a "guard" and the function relating the system state before the transition to the state after as the corresponding "reset". Variables used are described in Table I.

TABLE I

VARIABLES OF THE QUADROTOR WITH LOAD SYSTEM

$\mathcal{I}$, $\mathcal{B}$	World frame, body frame of the quadrotor
$m_Q, m_L, l \in \mathbb{R}$	Mass of quadrotor, load, length of cable
$\mathbb{I}$	Inertia tensor of quadrotor
$f \in \mathbb{R}$	Magnitude of thrust on quadrotor
$\mathbf{M} \in \mathbb{R}^3$	Moment vector on quadrotor, in $\mathcal{B}$
$\mathbf{x}_Q, \mathbf{x}_L \in \mathbb{R}^3$	Position vector of quadrotor, load, in $\mathcal{I}$
$\mathbf{p} \in \mathbb{S}^2$	Unit vector from quadrotor to load, in $\mathcal{I}$
$\omega \in \mathbb{R}^3$	Angular velocity of load, in $\mathcal{I}$
$R \in SO(3)$	Rotation matrix of quadrotor from $\mathcal{B}$ to $\mathcal{I}$
$\Omega \in \mathbb{R}^3$	Angular velocity of quadrotor, in $\mathcal{B}$

A. Quadrotor-With-Load Dynamics

This subsystem evolves on $\mathbb{S}^2 \times SE(3)$, with:

$$\mathbf{x}_1 = [\mathbf{x}_L \quad \dot{\mathbf{x}}_L \quad \mathbf{p} \quad \omega \quad R \quad \Omega]$$

Using a coordinate-free representation of the states and applying the extended Hamilton's principle with variations on the configuration manifold [6], we obtain the dynamics:

$$\frac{d}{dt}\mathbf{x}_L = \dot{\mathbf{x}}_L \tag{1}$$

$$(m_Q + m_L)(\ddot{\mathbf{x}}_L + g\mathbf{e}_3) = (\mathbf{p} \cdot fR\mathbf{e}_3 - m_Q l(\dot{\mathbf{p}} \cdot \dot{\mathbf{p}}))\mathbf{p} \tag{2}$$

$$\dot{\mathbf{p}} = \omega \times \mathbf{p} \tag{3}$$

$$m_Q l\dot{\omega} = -\mathbf{p} \times fR\mathbf{e}_3 \tag{4}$$

$$\dot{R} = R\hat{\Omega} \tag{5}$$

$$\dot{\Omega} = [\mathbb{I}]_{\mathcal{B}}^{-1}(\mathbf{M} - \Omega \times [\mathbb{I}]_{\mathcal{B}}\Omega) \tag{6}$$

B. Quadrotor Dynamics

The quadrotor subsystem evolves on $\mathbb{R}^3 \times SE(3)$, with:

$$\mathbf{x}_2 = [\mathbf{x}_L \quad \dot{\mathbf{x}}_L \quad \mathbf{x}_Q \quad \dot{\mathbf{x}}_Q \quad R \quad \Omega]$$

The quadrotor control inputs are the applied thrust f in the $\mathbf{b}_3$ direction and the moment $\mathbf{M}$ about the body frame axes. Applying the Newton-Euler equations to the quadrotor and assigning the projectile motion equation to the load gives :

$$\frac{d}{dt}\mathbf{x}_L = \dot{\mathbf{x}}_L \tag{7}$$

$$\ddot{\mathbf{x}}_L = -g\mathbf{e}_3 \tag{8}$$

$$\frac{d}{dt}\mathbf{x}_Q = \dot{\mathbf{x}}_Q \tag{9}$$

$$\ddot{\mathbf{x}}_Q = \frac{f}{m_Q}R\mathbf{e}_3 - g\mathbf{e}_3 \tag{10}$$

$$\dot{R} = R\hat{\Omega} \tag{11}$$

$$\dot{\Omega} = [\mathbb{I}]_{\mathcal{B}}^{-1}(\mathbf{M} - \Omega \times [\mathbb{I}]_{\mathcal{B}}\Omega) \tag{12}$$

C. Guards and Resets

The transition from subsystem 1 to 2 occurs when the cable tension becomes zero. We can explicitly express the tension force from Newton's equation for the load:

$$m_L\ddot{\mathbf{x}}_L = -T\mathbf{p} - m_L g\mathbf{e}_3 \tag{13}$$

$$T = m_L\|g\mathbf{e}_3 + \ddot{\mathbf{x}}_L\| \tag{14}$$

The transition from subsystem 2 back to 1 occurs when the quadrotor and the load are exactly a cable-length apart.

The reset from subsystem 1 to 2 is an identity map incorporating constraints $\mathbf{x}_Q = \mathbf{x}_L - l\mathbf{p}$, $\dot{\mathbf{x}}_Q = \dot{\mathbf{x}}_L - l\dot{\mathbf{p}}$. When the quadrotor regains contact with the load, the objects' positions remain the same while their change in velocity is modeled as a completely inelastic collision and with $m_Q >> m_L$.

D. Control

We use the controller presented by Sreenath et al. [6] to track desired load trajectories in the quadrotor-with-load subsystem and the controller proposed by Lee et al. [11] to track desired quadrotor trajectories in the quadrotor subsystem. Both these geometric controllers have almost global stability properties, allowing us to plan aggressive trajectories.

III. TRAJECTORY GENERATION BASICS

This section describes our general framework, which has previously been used to generate quadrotor trajectories [8].

A. Differential Flatness

A differentially flat system [12] is a system whose states and inputs can be expressed as smooth functions of a set of flag outputs and their derivatives. A hybrid system is differentially flat [6] if each subsystem is differentially flat, all guards are functions of their subsystems' flat outputs, and resets are smooth functions between flat outputs. Any sufficiently smooth trajectory in the flat outputs can be mapped into a dynamically feasible trajectory for the full system states. This low-dimensional flat space has dynamically uncoupled states, making it easier plan in than the full high-dimensional, dynamically coupled state-space.

Sreenath et al. [6] show that a quadrotor with a cable-suspended load is a differentially flat hybrid system. $\mathbf{y}_1 = [\mathbf{x}_L \quad \psi]^T$ are the flat outputs for subsystem 1, and $\mathbf{y}_2 = [\mathbf{x}_Q \quad \psi]^T$ are those for subsystem 2, where ψ is the quadrotor yaw. To see this result, rearrange (13) to express $\mathbf{p}$ with $\ddot{\mathbf{x}}_L$:

$$\mathbf{p} = \frac{-(\ddot{\mathbf{x}}_L + g\mathbf{e}_3)}{\|\ddot{\mathbf{x}}_L + g\mathbf{e}_3\|} \tag{15}$$

This provides the position of the quadrotor:

$$\mathbf{x}_Q = \mathbf{x}_L - l\mathbf{p} = \mathbf{x}_L + l\frac{(\ddot{\mathbf{x}}_L + g\mathbf{e}_3)}{\|\ddot{\mathbf{x}}_L + g\mathbf{e}_3\|} \tag{16}$$

Ultimately, in subsystem 1, the moment input is a function of $\mathbf{x}_L^{(6)}$ and in subsystem 2, the moment is a function of $\mathbf{x}_Q^{(4)}$.

B. Mixed Integer Quadratic Program Formulation

Given a series of n_w waypoint constraints, each dictating a feasible position or higher derivative value at a specified time, we seek a trajectory $\mathbf{x}(t) \in \mathbb{R}^3$ that satisfies the constraints while minimizing the cost functional:

$$J = \int_{t_0}^{t_f} \left\| \frac{d^r\mathbf{x}(t)}{dt^r} \right\|^2 dt \tag{17}$$

Let $P_i(t)$, $i = 1, 2, ..., n$, be a set of basis functions. Let the waypoint constraints occur at times $t_{des} = [t_0 \;\; t_1 \;\; ... \;\; t_m]$ with values $x_{des}^{(k)}(t_j)$, where multiple derivative values can be

specified at each t_j. In each dimension, we seek a smooth curve that is a linear combination of the basis functions:

$$x(t) = \begin{cases} x_1(t) = \sum_{i=1}^{n} c_{1,i} P_i(t) + c_{1,0}, & t_0 \le t < t_1 \\ x_2(t) = \sum_{i=1}^{n} c_{2,i} P_i(t) + c_{2,0}, & t_1 \le t < t_2 \\ \dots \\ x_m(t) = \sum_{i=1}^{n} c_{m,i} P_i(t) + c_{m,0}, & t_{m-1} \le t < t_m \end{cases} \tag{18}$$

To represent $\mathbf{x}(t) = [x(t) \;\; y(t) \;\; z(t)]$, we concatenate the vectors of coefficients for each dimension:

$$\mathbf{c} = [c_{x,1,n} \;\; c_{x,1,n-1} \;\; \dots \;\; c_{x,m,0} \;\; c_{y,1,n} \;\; \dots \;\; c_{z,m,0}]$$

and formulate the Quadratic Program (QP):

$$\begin{aligned} &\underset{\mathbf{c}}{\text{minimize}} \; J = \mathbf{c}^T Q \mathbf{c} \\ &\text{subject to } A\mathbf{c} = \mathbf{b} \end{aligned} \tag{19}$$

Q is a symmetric, square matrix corresponding to the cost functional (17). The constraint $A\mathbf{c} = \mathbf{b}$ imposes the waypoint constraints. It also contains continuity constraints at times when trajectory segments meet, forcing each dimension's trajectory to be continuous through the $(r-1)^{st}$ derivative.

Suppose there are n_o known convex obstacles with $n_f(o)$ faces each. Let $\mathbf{n}_{f,o}$ be the outwards unit normal of face f of obstacle o and $\mathbf{s}_{f,o}$ be a point on the face. We constrain the position at sample time t_s outside this face with:

$$(\mathbf{x}(t_s) - \mathbf{s}_{f,o}) \cdot \mathbf{n}_{f,o} \ge 0 \tag{20}$$

This constraint is linear with respect to $\mathbf{x}$. An obstacle is avoided if (20) is true for at least one of its faces. A set of binary variables $b_{s,f,o}$ can express this:

$$b_{s,f,o} \rightarrow (\mathbf{x}(t_s) - \mathbf{s}_{f,o}) \cdot \mathbf{n}_{f,o} \ge 0 \tag{21}$$

$$\sum_{i=1}^{n_f(o)} b_{s,i,o} \ge 1 \tag{22}$$

IV. Problem Formulation

For our system, assume waypoint specifications and obstacle locations are given. We seek a smooth trajectory that:

1) Satisfies the desired waypoint constraints
2) Guarantees collision avoidance with obstacles
3) Properly transitions between subsystems if necessary

The cable between the load and quadrotor should be taut whenever possible, thus, we first design a trajectory in the flat space of the quadrotor-with-load subsystem and plan transitions into the quadrotor subsystem only when necessary. Since the yaw angle of the quadrotor does not affect the load actuation, the focus of our problem is designing a load trajectory $\mathbf{x}_L(t)$. We use a polynomial basis and define the cost functional (17) with $r = 6$, as the moment input is a function of the 6^{th} derivative of the load trajectory.

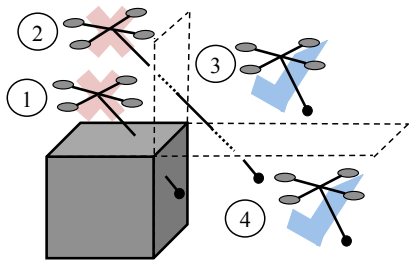

Fig. 2. Orientations of the load and quadrotor with respect to an obstacle's faces. In configuration 1, the load and the quadrotor do not collide with the obstacle, but the cable does. In configurations 3 and 4, the load and quadrotor are outside the same faces and the cable cannot collide with the obstacle corner. The constraint is conservative, in that it also precludes collision-free configurations like configuration 2.

A. Waypoint Constraints

To satisfy criteria 1, we formulate waypoint and continuity constraints $A\mathbf{c} = b$ as in (19). Additionally, the minimum load acceleration occurs when the load is in projectile motion. We choose n_{sL} sample times along each trajectory segment and, at each time t_s, impose the constraint:

$$\ddot{\mathbf{x}}_L(t_s) \cdot \mathbf{e}_3 + g \ge 0 \tag{23}$$

The angle ϕ_L between the cable and the vertical axis can be derived from (15):

$$\cos(\phi_L) = \frac{\ddot{\mathbf{x}}_L(t_s) \cdot \mathbf{e}_3 + g}{\|\ddot{\mathbf{x}}_L + g\mathbf{e}_3\|} \tag{24}$$

Thus, (23) also constrains $-\frac{\pi}{2} \le \phi_L \le \frac{\pi}{2}$.

B. Obstacle Avoidance Constraints

To satisfy criteria 2 for the load, we can directly use (20) to linearly constrain the load position at each sample time:

$$(\mathbf{x}_L(t_s) - \mathbf{s}_{f,o}) \cdot \mathbf{n}_{f,o} \ge d, \tag{25}$$

where $d \ge 0$ is defined later. We over-approximate the quadrotor a prism, with sides l_x, l_y, l_z, in which the vehicle can assume arbitrary orientation. We constrain this prism outside a face with:

$$(\mathbf{x}_Q(t_s) - \mathbf{s}_{f,o}) \cdot \mathbf{n}_{f,o} \ge |[l_x \;\; l_y \;\; l_z] \cdot \mathbf{n}_{fo}| \tag{26}$$

Using (16), (26) can be expressed in the flat variables:

$$\left(\mathbf{x}_L(t_s) + l\frac{\ddot{\mathbf{x}}_L(t_s) + g\mathbf{e}_3}{\|\ddot{\mathbf{x}}_L(t_s) + g\mathbf{e}_3\|}\right) \cdot \mathbf{n}_{f,o} \ge s_{f,o} + \gamma_{f,o}, \tag{27}$$

where $s_{f,o} = \mathbf{s}_{f,o} \cdot \mathbf{n}_{f,o}$ and $\gamma_{f,o} = |[l_x \;\; l_y \;\; l_z] \cdot \mathbf{n}_{fo}|$.

1) Linear Over-Approximation: We incorporate the non-linear constraint (27) through a piecewise linear over-approximation. From (26):

$$l\mathbf{p}(t_s) \cdot \mathbf{n}_{f,o} \le \mathbf{x}_L(t_s) \cdot \mathbf{n}_{f,o} - s_{f,o} - \gamma_{f,o} \tag{28}$$

Given (25), (28) will hold if:

$$l\mathbf{p}(t_s) \cdot \mathbf{n}_{f,o} \le d - \gamma_{f,o} \tag{29}$$

We partition the valid configuration space into three regions and use binary variables to enforce that the system must be in one of these regions for at least one obstacle face. These equations are stated in (32)-(34). Note this determines d.

At each sample time, obstacle avoidance constraints must be satisfied for at least one face of each obstacle. We further require them to be satisfied with respect to the same faces so the cable does not "nick" obstacles, as illustrated in Fig. 2.

C. Hybrid System

To allow subsystem transitions, we assign a state r_j to each trajectory segment j, where the system is in the quadrotor-with-load subsystem if $r_j = 0$ and the quadrotor subsystem if $r_j = 1$. Assume these assignments are known a priori. For segments where $r_j = 0$, (32)-(34) ensure collision avoidance. However, we allow for these segments' sample points to be in the quadrotor subsystem, presumably after a subsystem transition. At these times, we only impose load collision avoidance constraints and defer quadrotor trajectory planning. In this subsystem, the load must be in free-fall, so we accordingly constrain the acceleration and higher derivatives as in (35). For segments where $r_j = 1$, the load trajectory must be the projectile motion equation. Since our basis functions are polynomials, we can directly constrain the coefficients using linear equations (31).

V. Trajectory Planning Algorithm

We plan the load trajectory, state designations r_j, and necessary quadrotor trajectories with the following steps:

1) Solve for an initial load trajectory.
2) Refine the load trajectory and add any necessary zero-tension segments.
3) Generate corresponding quadrotor trajectories.

We detail each step in the following sections.

A. Initial Load Trajectory Planning

The complete decision vector for the load trajectory MIQP is $\mathbf{d} = [\mathbf{c}\ \ \mathbf{b}]$. $\mathbf{c}$ is the vector of trajectory coefficients and $\mathbf{b}$ is the vector of integer variables, where $b_{\beta;j,s,f,o}, \beta = 1, 2, 3, 4$ corresponds to the sample at t_s of segment j with respect to face f of obstacle o. Explicitly, the optimization problem is:

$$\underset{\mathbf{d}}{\text{minimize}}\ J = \int_{t_0}^{t_m} \left\| \frac{d^6 \mathbf{x}_L(t)}{dt^6} \right\|^2 dt \tag{30}$$

subject to:

Waypoint constraints: $A\mathbf{c} = b$

Inequality constraints: $\ddot{\mathbf{x}}_L(t_s) \cdot \mathbf{e}_3 + g \geq 0$

State constraints:

$$\forall j \text{ such that } r_j = 1, \begin{cases} c_{x,j,k} = 0\ \forall k = 2, ..., n \\ c_{y,j,k} = 0\ \forall k = 2, ..., n \\ c_{z,j,k} = 0\ \forall k = 3, ..., n \\ c_{z,j,2} = -\frac{g}{2} \end{cases} \tag{31}$$

Obstacle avoidance constraints:

$$b_{1;j,s,f,o} \rightarrow \begin{cases} \mathbf{x}_L(t_s) \cdot \mathbf{n}_{f,o} \geq s_{f,o} + \gamma_{f,o} \\ \mathbf{x}_L(t_s) \cdot \mathbf{n}_{f,o} \leq s_{f,o} + \gamma_{f,o} + l \\ \ddot{\mathbf{x}}_L(t_s) \cdot \mathbf{n}_{f,o} \geq -g\mathbf{e}_3 \cdot \mathbf{n}_{f,o} \end{cases} \tag{32}$$

$$b_{2;j,s,f,o} \rightarrow \begin{cases} \mathbf{x}_L(t_s) \cdot \mathbf{n}_{f,o} \geq s_{f,o} + \gamma_{f,o} + D_{min,f,o} \\ \mathbf{x}_L(t_s) \cdot \mathbf{n}_{f,o} \leq s_{f,o} + \gamma_{f,o} + l \\ -(l\ddot{\mathbf{x}}_L(t_s) \cdot \mathbf{n}_{f,o} + D_{min,f,o}\ddot{\mathbf{x}}_L(t_s) \cdot \mathbf{e}_3) \leq \\ \qquad g(l\mathbf{e}_3 \cdot \mathbf{n}_{f,o} + D_{min,f,o}) \end{cases} \tag{33}$$

$$b_{3;j,s,f,o} \rightarrow \mathbf{x}_L(t_s) \cdot \mathbf{n}_{f,o} \geq s_{f,o} + \gamma_{f,o} + l \tag{34}$$

$$b_{4;j,s,f,o} \rightarrow \begin{cases} \mathbf{x}_L(t_s) \cdot \mathbf{n}_{f,o} \geq s_{f,o} \\ \ddot{\mathbf{x}}_L(t_s) = [0\ \ 0\ \ -g] \\ \mathbf{x}_L^{(k)}(t_s) = [0\ \ 0\ \ 0]\ \forall k = 3, ..., r-1 \end{cases} \tag{35}$$

$$\sum_{f=1}^{n_f(o)} \sum_{\beta=1}^{4} b_{\beta;j,s,f,o} \geq 1 \tag{36}$$

$D_{min,f,o} = l\cos(\Delta\phi)$, where $\Delta\phi = \phi_n - \phi_{L,max}$ bounded by $-\frac{\pi}{2} \leq \Delta\phi \leq \frac{\pi}{2}$, ϕ_n is the angle between $\mathbf{n}_{f,o}$ and the vertical, and $\phi_{L,max}$ is a chosen maximum load angle.

For an initial load trajectory, we assume $r_j = 0$ for all segments. Thus, (31) is not used in this step. However, the inclusion of (35) still allows for the existence of zero-tension segments. These segments will be found in the following load trajectory refinement step.

B. Load Trajectory Refinement

The initial load trajectory might contain time periods where $\ddot{z}_L = -g + \epsilon$, $\epsilon << 1$. This will occur when $b_{4;j,s,f,o} = 1$ for consecutive sample points, indicating the need for a zero-tension segment. Physically, when $\ddot{z}_L$ is close to $-g$, if $\ddot{x}_L$ and $\ddot{y}_L$ are nonzero, the quadrotor is commanded to pull the load exactly horizontal. If $\ddot{x}_L = \ddot{y}_L = 0$, the system is kept "right before" it fulfills the guard condition. While these solutions satisfy our problem numerically, they are not practical. Physical limitations, such as motor and actuator limits and friction forces, will easily perturb the cable into the zero-tension state. To eliminate this instability, we simply insert a planned zero-tension trajectory segment.

We numerically approximate the set of times t_a, where such segments begin, and t_b, where they end. Note that these times do not have to coincide with the waypoint constraint times. We insert these times into the original desired time vector to force a trajectory segment that begins and ends at each pair of t_a and t_b. We designate $r_j = 1$ for the corresponding segments and solve a new MIQP that incorporates all previous constraints, but imposes (31) on the necessary segments.

C. Quadrotor Trajectory Planning

For each zero-tension segment, we plan a corresponding quadrotor trajectory in subsystem 2's flat space. Let t_a and t_b be the begin and end times of the zero-tension segment. We derive boundary conditions on the quadrotor position to its third derivative from differential flatness. We formulate obstacle avoidance constraints using integer variables at n_{sQ} sample times. We also must keep the quadrotor from colliding with the load:

$$\|\mathbf{x}_Q(t_s) - \mathbf{x}_L(t_s)\| \geq \max(l_x, l_y, l_z)$$

Since this constraint is nonconvex, we explicitly restrict the quadrotor to be above the load in the z direction:

$$(\mathbf{x}_Q(t_s) - \mathbf{x}_L(t_s)) \cdot \mathbf{e}_3 \geq l_z + \delta, \tag{37}$$

where $\delta > 0$ is a minimum clearance. Further, we constrain the quadrotor from pulling the cable taut before the planned zero-tension segment ends:

$$\|\mathbf{x}_Q(t_s) - \mathbf{x}_L(t_s)\| \leq l \tag{38}$$

$\mathbf{x}_L(t)$ is known. Eq. 38 is a convex quadratic constraint, making the quadrotor trajectory generation a MIQCP. To allow for load releases, we omit (38) in the final segment.

The decision vector is $\mathbf{d}_Q = [\mathbf{c}_Q \quad \mathbf{b}_Q]$. $\mathbf{c}_Q$ is the vector of trajectory coefficients. $\mathbf{b}_Q$ is the vector of obstacle avoidance binary variables. Here, the quadrotor position is a flat variable, and (26) becomes linear. Since the moment input is a function of the quadrotor's 4^{th} derivative, we find minimum snap trajectories. The full problem is:

$$\underset{\mathbf{d}_Q}{\text{minimize}}\ J = \int_{t_0}^{t_m} \left\| \frac{d^4\mathbf{x}_Q(t)}{dt^4} \right\|^2 dt \tag{39}$$

subject to:

Waypoint constraints: $A\mathbf{c}_Q = b$

Obstacle avoidance constraints:

$$b_{s,f,o} \rightarrow \mathbf{x}_Q(t_s) \cdot \mathbf{n}_{f,o} \geq s_{f,o} + \gamma_{f,o}$$
$$\sum_{f=1}^{n_f(o)} b_{s,f,o} \geq 1$$

Collision avoidance constraints:

$$\mathbf{x}_Q(t_s) \cdot \mathbf{e}_3 \geq l_z + \delta + \mathbf{x}_L(t_s) \cdot \mathbf{e}_3$$
$$\|\mathbf{x}_Q(t_s) - \mathbf{x}_L(t_s)\|^2 \leq l^2, \text{ if necessary}$$

D. Complexity Analysis

The algorithm runtime is dominated by the MIQP for the load trajectory. Given n basis functions, m segments, n_{sL} sample times per segment, the decision vector $\mathbf{d}$ is size:

$$n_d = 3mn + 4mn_{sL}\sum_{i=1}^{n_o} n_f(i).$$

The first term contains coefficient variables and the second contains obstacle avoidance integer variables. The decision vector grows quickly: a new obstacle adds $4mn_{sL}n_f(o)$ integer variables and an additional sample time adds $4m\sum_{i=1}^{n_o} n_f(i)$ variables.

To limit this effect, we initially choose a small number of sample points. We then check the resulting solution at n_c sample points for collisions, where n_c is large, and increase n_{sL} if collisions are found. Verifying a solution requires mn_cn_o collision checks. However, collision checking is a constant time process and most problems require only 5-10 sample points for a collision free solution. On the other hand, we solve the MIQP with a branch and bound solver, where the number of iterations increases exponentially with the number of binary variables. Thus, solving multiple MIQP problems with fewer sample points and validating each solution proves more practical than oversampling.

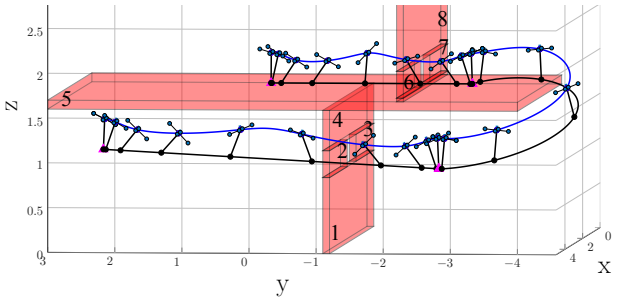

Fig. 3. Maneuvering through window-like obstacles

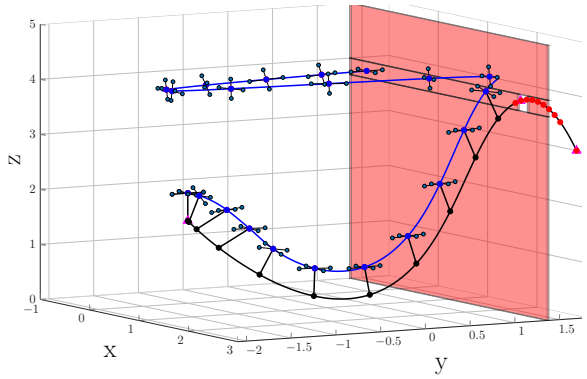

Fig. 4. Trajectory with load release

We also preprocess the problem by partitioning the Euclidean space into regions and solving a separate trajectory generation problem within each region. We impose homogenous boundary constraints at the boundary of each region to ensure continuity between trajectories. This allows us to ignore obstacles that are far away or behind other obstacles. Section VI discuses an example of this partitioning.

Finally, a poorly designated desired time between waypoint constraints could result in unpredictable solutions. Future work could incorporate an optimization of these time intervals between waypoints, for example with a gradient descent search.

VI. Numerical Results

In this section, we present representative numerical results. We solve the optimization problems using IBM's CPLEX optimizer in Matlab on a 2.5GHz Intel Core i7 Macbook Pro. We chose $n = 11$ polynomial basis functions.

A. Obstacle Avoidance

The example shown in Fig. 3 demonstrates planning for obstacle avoidance. The system maneuvers through two window obstacles of height 0.3m with cable length $l = 0.34$m. We include $m = 14$ segments and $n_{sL} = 1$-4 sample points per segment. There are four specified waypoint positions, where all higher derivatives are constrained to 0.

Triangles in Fig. 3 show the designated positions. We partition the space into three separate problems. In the first, moving from position 1 to 2, we consider only obstacles

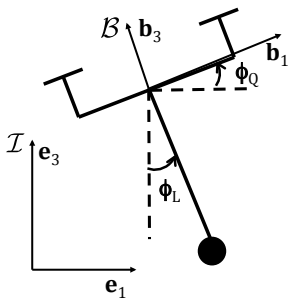

(a) Planar quadrotor model

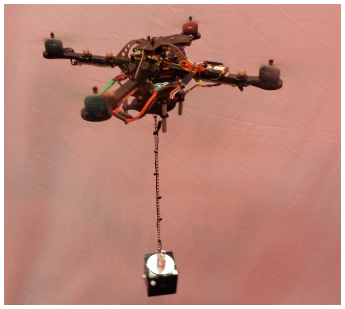

(b) Electromagnet mechanism

Fig. 5. Quadrotor with cable-suspended load

1-5, as moving below obstacle 5 guarantees avoidance of obstacles 6-8. In the second problem, we move from position 2 to 3 and consider only obstacle 5. In the third, we consider obstacles 5-8 when moving from position 3 to 4.

The resulting solution is pictured in Fig. 3. The initial load trajectory solution was found in 3277.63s. The system always remains in the quadrotor-with-load subsystem, so trajectory refinement is not necessary. Note the two qualitatively different maneuvers: because of the y-positions of the two windows, the load leads the quadrotor through the first while it follows the quadrotor through the second.

B. Hybrid Trajectories

The ability to plan transitions between subsystems allows us to execute otherwise infeasible tasks. Example 3 illustrates one scenario, where the load is thrown through a window too small for the quadrotor to pass. This problem is formulated with $m = 5$ segments and $n_{sL} =$ 0-5 sample points each. $t_{des} = [0 \;\; 0.6 \;\; 1.2 \;\; 1.8 \;\; 2.4 \;\; 2.9]$, with positions specified at $t_0 = 0$, $t_4 = 2.4$, $t_2 = 2.9$. We only constrain the 3^{rd} to $(r-1)^{st}$ derivatives to 0 (omitting constraints on acceleration) to make a free-fall trajectory feasible.

In the initial load trajectory, we assume $r_j = 0$ for all segments. However, at all sample times in segment 5, $b_{4;5,s,f,o} = 1$ for some face of each obstacle, constraining $\ddot{z}_L$ at these times to $-g$. In the refinement step, we identify $t_a = 2.3$ and $t_b = 2.9$ as times between which $\ddot{z}_L = -g + \epsilon$ for $\epsilon = 0.03$m/s/s. In our refined MIQP, $t_{des} = [0 \;\; 0.6 \;\; 1.2 \;\; 1.8 \;\; 2.3 \;\; 2.4 \;\; 2.9]$, $r_5 = r_6 = 1$. Thus, we add (31) as constraints for segments 5 and 6. Finally, we find the corresponding quadrotor trajectory using an arbitrary final position. Fig. 4 illustrates the solution, found in 108.55s.

VII. Experimental Results

We conducted experiments on a Hummingbird quadrotor from Ascending Technologies[1] using a Vicon motion capture system[2] for state information. Fig. 5b pictures the quadrotor with a box load suspended from a 0.34 meter cable. For experiments, we approximate the system as a planar system, with states shown in Fig. 5a.While this model is a simplification of the full system dynamics, it is a crucial step towards developing an understanding of the hybrid system.

[1]http://www.asctec.de
[2]http://www.vicon.com

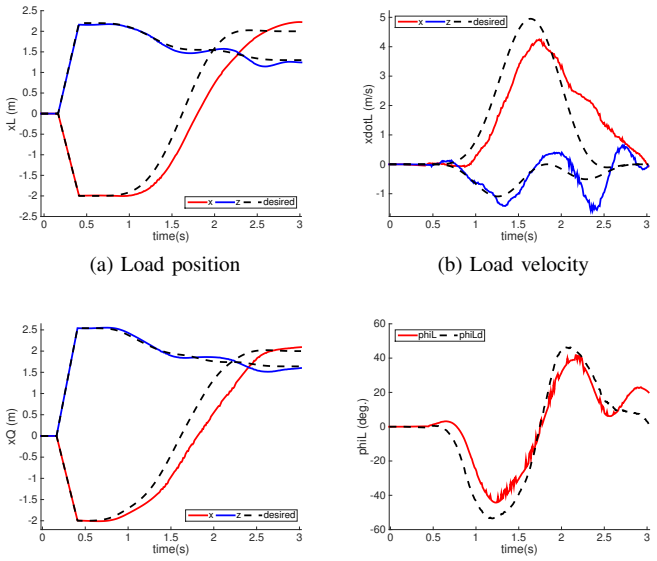

(a) Load position (b) Load velocity

(c) Quadrotor position (d) Load angle

Fig. 6. State tracking in obstacle avoidance maneuver

Video of these results can be found at `http://youtu.be/qO4MsiuLCoc`.

A. Obstacle Avoidance

We first maneuver the quadrotor and load through a window, where the height of the window is too short for the system to pass through with the load hanging vertically. The obstacle is represented as two rectangles and inflated for additional safety. We use $n = 11$ polynomial basis functions, $m = 4$ trajectory segments, and $n_{sL} = 4$ samples per segment. Waypoint constraints are enforced at $t_0 = 0$s with load position $\mathbf{x}_L(t_0) = [-2 \;\; 1.9]^T$ and higher derivatives zero and at $t_4 = 2.6$s with load position $\mathbf{x}_L(t_4) = [2 \;\; 1.9]^T$ and again, higher derivatives zero.

Fig. 7 shows snapshots of the maneuver, and Fig. 6 displays tracking of the trajectory. The system always remains in the quadrotor-with-load subsystem. The load is swung forward to a maximum angle of 40^o from the vertical to pass through the window. Unfortunately, the tracking error is significant. One possible cause is that while we control the quadrotor position to a fixed y plane, it is impossible to constrain the load swing to the plane. In this fast maneuver, the out-of-plane motion of the swinging load is significant. Future work will focus on extending the controller to the full 3D case and reducing these tracking errors.

B. Load Pick-up and Release with a Hybrid Trajectory

We additionally demonstrate the complete hybrid dynamical system. The quadrotor executes an elliptical trajectory, picking up the load at a $\mathbf{x}_L = [-0.80 \;\; 0.81]^T$ and releasing it at $\mathbf{x}_L = [1 \;\; 1.2]^T$ at an angle of 20^o from the vertical. We manipulate the load using the electromagnet pictured in Fig. 5b. We use trigonometric basis functions to obtain an iterative maneuver.

We use the motion capture system to detect subsystem transitions. For load pick-up, we require that the distance

Fig. 7. Quadrotor moving through window

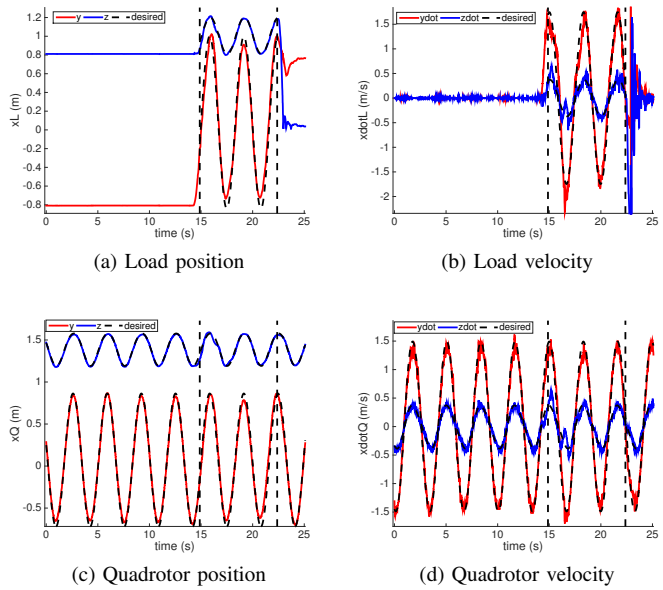

(a) Load position (b) Load velocity

(c) Quadrotor position (d) Quadrotor velocity

Fig. 8. State tracking in load-transport maneuver

between the quadrotor and load be the cable length for 0.8s before switching controllers. This delay verifies that the load was successfully picked up and avoids false switches during failed attempts. The load is released when its state is within 0.05m of its desired release position and 0.02m/s of its desired release velocity. In this case, the switch between controllers happens instantaneously, as there are no false releases. Future designs could use an on-board force sensor to remove reliance on the motion capture system.

Fig. 8 displays tracking results, with black vertical lines indicating transition points between tracking the quadrotor position in the quadrotor subsystem and the load position in the quadrotor-with-load subsystem. We see through Figs. 8c-8d that we are able to maintain continuity in the quadrotor states at the transition points without significant increase in tracking error. Because there is some initial error in the load state at pick-up, the elliptical trajectory is repeated twice before the load state converges to the desired drop conditions. This can be seen in Figs. 8a - 8b. In this maneuver, the load angle and quadrotor attitude both reach angles of 20^o and the load velocity reaches almost 2m/s.

VIII. Conclusions

We propose a trajectory planning algorithm for a quadrotor with a cable-suspended payload modeled as a hybrid dynamical system. Numerical and experimental results indicate that the method is practical for generating trajectories that include aggressive obstacle avoidance maneuvers and hybrid state transitions. Our future work is directed toward speeding up computations by optimizing our implementation and independently iterating over each segment of the trajectory, addressing the stability of the hybrid system (beyond the stability of individual systems), and applications to multi-robot manipulation.

Acknowledgment

We would like to thank Koushil Sreenath for many insightful discussions and Terry Kientz for the design and fabrication of our quadrotor's electromagnet mechanism.

References

[1] J. Thomas, J. Polin, K. Sreenath, and V. Kumar, "Avian-inspired grasping for quadrotor micro UAVs," in *ASME International Design Engineering Technical Conference (IDETC)*, 2013.

[2] J. Thomas, G. Loianno, K. Sreenath, and V. Kumar, "Toward Image Based Visual Servoing for Aerial Grasping and Perching," in *IEEE International Conference on Robotics and Automation (ICRA)*, 2014.

[3] M. Bernard and K. Kondak, "Generic slung load transportation system using small size helicopters," in *IEEE International Conference on Robotics and Automation (ICRA)*, 2009.

[4] A. Faust, I. Palunko, P. Cruz, R. Fierro, and L. Tapia, "Learning swing-free trajectories for UAVs with a suspended load," in *IEEE International Conference on Robotics and Automation (ICRA)*, 2013.

[5] K. Sreenath, N. Michael, and V. Kumar, "Trajectory generation and control of a quadrotor with a cable-suspended load – a differentially-flat hybrid system," in *IEEE International Conference on Robotics and Automation (ICRA)*, 2013.

[6] K. Sreenath, T. Lee, and V. Kumar, "Geometric control and differential flatness of a quadrotor UAV with a cable-suspended load," in *IEEE Conference on Decision and Control (CDC)*, 2013.

[7] C. Richter, A. Bry, and N. Roy, "Polynomial trajectory planning for quadrotor flight," in *IEEE International Conference on Robotics and Automation (ICRA)*, 2013.

[8] D. Mellinger, A. Kushleyev, and V. Kumar, "Mixed-integer quadratic program trajectory generation for heterogeneous quadrotor teams," in *IEEE International Conference on Robotics and Automation (ICRA)*, 2012.

[9] R. Deits and R. Tedrake, "Footstep planning on uneven terrain with mixed-integer convex optimization," in *IEEE-RAS International Conference on Humanoid Robots*, November 2014.

[10] C. de Crousaz, F. Farshidian, and J. Buchli, "Aggressive optimal control for agile flight with a slung load," in *IEEE/RSJ International Conference on Intelligent Robots and Systems (IROS) Workshop on Machine Learning in Planning and Control of Robot Motion*, 2014.

[11] T. Lee, M. Leok, and N. H. McClamroch, "Control of complex maneuvers for a quadrotor UAV using geometric methods on SE(3)," in *Asian Journal of Control*, 2011.

[12] R. M. Murray, M. Rathinam, and W. Sluis, "Differential flatness of mechanical control systems: A catalog of prototype systems," in *ASME International Congress and Exposition*, 1995.